Chapter 7

Titanium Carbide (TiC) Production by Mechanical Alloying

Héctor Enrique Jaramillo Suárez,
Nelly Alba de Sanchez and Julian Arnaldo Avila Diaz

Additional information is available at the end of the chapter

http://dx.doi.org/10.5772/intechopen.76690

Abstract

This chapter presents the process for obtaining titanium carbides (TiC) from elemental powders of titanium dioxide, aluminum, and graphite by means of the mechanical alloying technique, using a semi-industrial attritor mill. Three grindings were performing: a wet, a dry, and a vacuum grinding. The mass relations between grinding elements and powders used were 20:1 to wet grinding and 40:1 to dry and vacuum grinding. Each grinding took 36 h with a control stop at 18 h. The samples were analyzed using X-ray diffraction analysis and the characteristics peak were detected on $2\theta = 41$, 60, 72, and 76°. Targets of TiC were produced using compaction and sintering processes. The particle size (between 200 nm and 1 μm) was measure using a scanning electron microscopy (SEM). After the milling process, the particle size showed a huge distribution. However, after the sintered process, the particle size (lower than 5 μm) distribution had a low dispersion and their shape trends to be spherical. It is necessary to highlight that the precursors used were low cost compared to the high cost and purity powders used for this purpose; so this method is an excellent alternative to implement as a low-cost industrial process.

Keywords: titanium carbide, mechanical alloy, mechanosynthesis, milling, sintering process

1. Introduction

Such metastable phases as solid supersaturated solutions without crystalline equilibrium or intermediate quasicrystalline stages and amorphous alloys can be synthesized by mechanical alloying [1, 2]. In addition, nanostructures with grain sizes of a few nanometers, usually

<100 nm, can be produced. These metastable phases characteristically have an interesting combination of physical, chemical, mechanical, and magnetic properties that are now being explored due to their potential applications [3].

Mechanically alloyed materials are used in a variety of industries. They are used in the synthesis and processing of advanced materials (magnetic, superconducting, and ceramic materials) such as intermetallic materials, nanocomposites, catalysts, hydrogen-storage materials, gas heaters and dampers, and modifiers of the solubility of organic compounds for waste management and fertilizer production [4]. However, the main industrial applications of mechanically alloyed materials have been in heat treatments, glass processing, energy production, and the aerospace industry.

When in the search for materials which meet increasingly strict requirements, such as high rigidity, high mechanical strength, and low density, such processes as powder technologies and mechanical alloying emerge. These processes do not have any limitations unlike conventional processes, for example, the melting process [5], which is not viable when there are materials with very different melting temperatures, low solubility limits, manufacturing costs due to high energy consumption, and environmental impact problems. In this respect, the mechanical alloying is a non-traditional technique, industrially competitive in obtaining composite materials, easy to use, low cost, and environmentally friendly [6]. This process produces alloys in solid state from elemental powders of any type of material [1], using the impact energy produced by milling elements.

The materials produced by mechanical alloying have a good thermal stability of their mechanical properties. The stability of the mechanical strength is due to the uniform dispersion (with a spacing range of 100 nm) with very fine oxide particles (5–50 nm), which are stable at high temperatures, and inhibit the movement of dislocations in the metallic matrix and increase the strength of the creep deformation alloy. Other characteristic is a fairly homogeneous distribution of the elements of the alloy during the mechanical alloying that gives rise to a solid solution (strengthening) and precipitation-hardening alloys with more stability at high temperatures and a general improvement of the mechanical properties.

The materials obtained by mechanical alloying also have excellent resistance to oxidation and corrosion, which is mainly due to the homogeneous distribution of the alloying elements and adhesion between particles [7, 8]. Due to these characteristics, these materials are widely used in aerospace applications [9], where materials with high mechanical performance are generally needed, due to the unfavorable conditions of use.

In this sense, this chapter presents the process for obtaining titanium carbides (TiC) at a laboratory level. The TiC was obtained from elemental powders of titanium dioxide, aluminum, and graphite by means of the mechanical alloying technique, using a semi-industrial capacity attritor mill.

2. Experimental data

2.1. Initial hypothesis

To obtain titanium carbides, a chemical analysis was conducted:

$$TiO_2 + C + Al \rightarrow TiC + Al_2O_3 \tag{1}$$

http://dx.doi.org/10.5772/intechopen.76690

On performing the balancing of Eq. (1), we have.

$$3TiO_2 + 3C + 4Al \rightarrow 3TiC + 2Al_2O_3 \tag{2}$$

From Eq. (2), the molar mass of the elements involved in the reaction was determined and the weight of the powders involved in the mechanical alloying process was calculated (**Table 1**). The percentage of participation for each initial powder was calculated as.

$$\%\text{Re}activo = \frac{W}{W_t} x100\% \tag{3}$$

where W is the weight of the reactive powder and W_t is the total weight of the reagent.

So,

$$\%TiO_2 = \frac{239.7}{383.7} x100\% = 62.4\% \tag{4}$$

$$\%C = \frac{36.0}{383.7} x100\% = 9.4\% \tag{5}$$

$$\%Al = \frac{108.0}{383.7} x100\% = 28.1\% \tag{6}$$

2.2. Milling characteristics

During the experimental process, three initial millings were made: two wet millings and one vacuum dry milling, in order to fine-tune the process parameters. Once the process parameters have been fine-tuned (**Table 2**), milling was performed to obtain the TiC.

Chemical element	Mass (g/mol)	Left side of Eq. (2)		Right side of Eq. (2)	
		Moles	Mass (g)	Moles	Mass (g)
Ti	47.9	3	143.7	3	143.7
O_2	16.0	3	96.0	3	36.0
C	12.0	3	36.0	2	108.0
Al	27.0	4	108.8	2	96.0
Total		13	383.7	10	383.7

Table 1. Balancing chemical.

Process	Grinding	Initial powders (g)	Ratio $M_{balls}/M_{powders}$	Pressure (Torr)	Velocity (rpm)	Grinding time (h)
Wet grinding	Grinding 1	500	20:1	6.7×10^2	250	5
	Grinding 2	250	40:1	6.7×10^2	300	7
Dry grinding	Grinding 3	250	40:1	8.0×10^{-3}	500	12

Table 2. Experimental process details of powder grinding.

2.2.1. The mill

To make the millings, an attritor-type ball mill was used; it was developed and built by Universidad Autónoma de Occidente for this purpose (www.uao.edu.co) (**Figure 1**). The bowl of the mill has a maximum capacity of 2 l and the impeller has a rotation speed of 500 rpm. The bowl has a torispherical lid and the assembly is able to withstand temperatures over 300°C and pressures of 1.72 MPa (175 psi), which ensures a protective atmosphere.

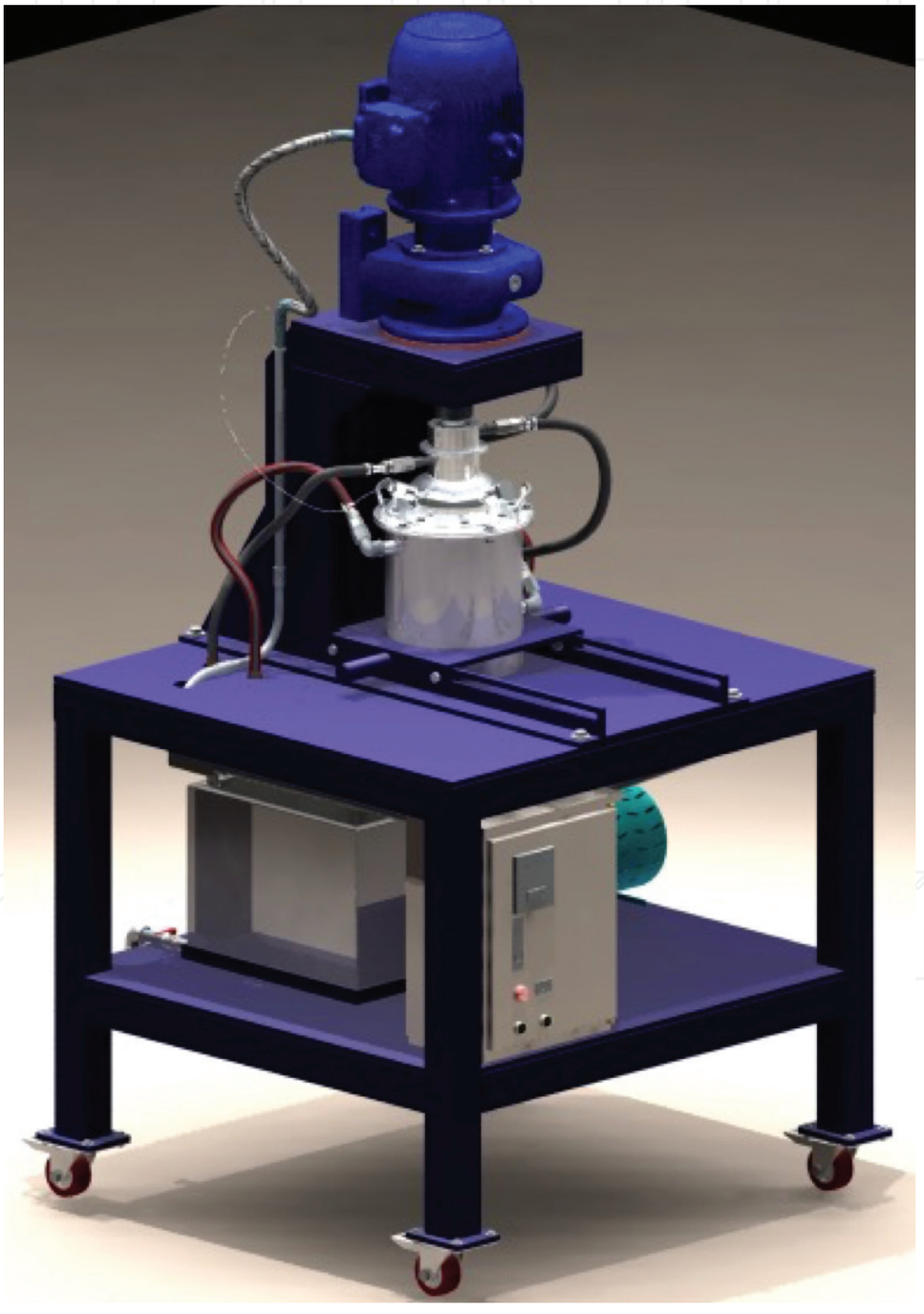

Figure 1. Attritor-type ball mill.

The mill also has a cooling system that allows the control of the internal temperature of the milling and a vacuum system with an Alcatel Adixen vacuum pump model 2005 SD for a vacuum pressure of 1 Pa and a 5.4 m^3/h flow. The alloy steel balls with a 10-mm-diameter were used. For more details of the design of the attritor mill, it is recommended to read Botero et al. [10].

For the milling 1-wet is called this way because 4% by weight of liquid ethanol was added as the process-controlling agent (PCA). The total amount of powders used in the milling was 500 and 20 g of ethanol (**Table 3**).

The M_{powder}/M_{balls} mass ratio determines the mass of balls that impact with regard to the mass of the powder material. At laboratory level, the recommended relationships [11] are between 10/1 and 20/1. For this milling, a ratio of 20/1 was selected, in order to have a greater amount of impact energy. Therefore, the mass of the balls (M_{balls}) is calculated as

$$\frac{M_{balls}}{M_{powder}} = \frac{20}{1} \Rightarrow M_{balls} = \frac{(2 \times 0.5\ \text{kg})}{1} = 10\ \text{kg} \tag{7}$$

For this milling, the agitator shaft speed was 250 rpm, the milling time was 5 h, and the process was conducted at an atmospheric pressure.

For the milling 2-wet, a total of 250 g of powder was used (**Table 4**); the most critical work parameters of the equipment were selected, in order to have the maximum available energy and ensure the formation of titanium carbide. Thus, 4% (10 g) by weight was added as the dispersing agent (PCA).

Material	Percentage (%)	Powders mass (g)
Titanium dioxide	62.47	312.35
Graphite	28.13	140.5
Aluminum	9.4	47.0
Total initial powder	100	500.0

Table 3. Amount and percentages of the initial powders of the wet grinding 1.

Material	Percentages (%)	Powders mass (g)
Titanium dioxide	62.47	156.2
Graphite	28.13	70.3
Aluminum	9.4	23.5
Total initial powder		250.0

Table 4. Amount and percentages of the initial powders of the wet grinding 2.

A mass ratio of 40/1 was used, for which a ball mass was obtained:

$$\frac{M_{balls}}{M_{powder}} = \frac{40}{1} \Rightarrow M_{balls} = \frac{(40 \times 0.5\ \text{kg})}{1} = 10\ \text{kg} \tag{8}$$

An agitator shaft speed of 300 rpm and a 7-h milling time at an atmospheric pressure was used.

For the milling 3-dry and vacuum, the amount of powder used in the milling was 250 g (**Table 5**). Aluminum powder was added in order to eliminate the formation of CO_2, to avoid the increase in pressure.

The mass ratio of 40/1 was used. For this case, the ball mass was

$$\frac{M_{balls}}{M_{powder}} = \frac{40}{1} \Rightarrow M_{balls} = \frac{(40 \times 0.25\ \text{kg})}{1} = 10\ \text{kg} \tag{9}$$

An agitator shaft speed of 500 rpm and a 12-h milling time were used, and the process was performed in vacuum. In this milling, ethanol was not added to the mixture as a dispersing agent.

From the initial millings, it was determined that the milling time had to be longer, in order to obtain higher concentrations of titanium carbide in the milling; this milling was named final milling. **Table 6** lists the parameters used in the milling.

2.3. Characterization of milling powders

The powders obtained from millings 1, 2, and 3 were characterized by X-ray diffraction with a Rigaku Rint 2200 diffractometer. The parameters used for X-ray diffraction analysis in millings 1 and 2 were 20 kW, 20 mAmp, and a sweep between 5 and 140° was performed with a scanning speed of 0.2 s/step. The parameters used for the analysis of milling 3 were 40 kW, 40 mAmp, a sweep between 10 and 100°, and a scanning speed of 2 s/step. For milling 3, three samples of material were taken in different parts of the milling container:

1. Sample 1: dust adhered to the milling spheres.
2. Sample 2: dust adhered to the walls of the bowl.
3. Sample 3: dust adhered to the bottom of the bowl.

Material	Percentage (%)	Powders mass (g)
Titanium dioxide	62.47	156.2
Graphite	28.13	70.3
Aluminum	9.4	23.5
Total initial powders	100	250

Table 5. Amount and percentages of the initial powders of the grinding 3, dry grinding, and vacuum grinding.

Process	Initial powders (g)	Temperature (°C)	Ratio $M_{balls}/M_{powders}$	Pressure (Torr)	Velocity (rpm)	Grinding time (h)
Grinding	169	38	40:1	1.7×10^{-2}	500	18
Grinding	169	38	40:1	1.7×10^{-2}	500	36

Table 6. Experimental process details of powders grinding.

The final milling was performed in a 36-h time; however, a stop of the process was made at 18 h to take a sample. For both cases, an X-ray analysis was performed, with a scanning speed between 1 and 5°/min, with a step of 0.020°, 40 kW, 40 mAmp, and a sweep between 10° and 100° (**Table 7**).

With the 36-h final milling powder, we proceeded to obtain three targets of 25.4-mm diameter, compacting and sintering them later (**Table 8**). In the compaction, a Carver hydraulic press with a maximum load capacity of 12 tons was used. A 10-ton load was applied for 3 min; in each process, the targets were between 4.5- and 6.5-mm thick.

The 5.0-mm thick target was divided into four parts in order to subject it to different sintering temperatures. The first part of the target and, according to the recommendations of Lü and Lai [12], the sample was put into the preheated oven at 700°C and kept at a sustained temperature for 1 h. After that, the oven was turned off and the material was let to cool down to room temperature inside the oven with the door closed. For the second part of the target, the process was repeated at a temperature of 1000°C. The two samples were then removed from the oven and a visual examination was performed.

Grinding	Composition	Abundance
18-h grinding	TiO_2	++
	TiC	+++
	SiO_3	+
	Al_2O_3	+
36-h grinding	TiO_2	++
	TiC	+++
	SiO_3	++
	Al_2O_3	+
	Fe	+

Convention: +++, abundant (>50%); ++, common (20–40%); ++, poor (10–20%); +, sparse (3–10%).

Table 7. Results of X-ray analysis.

Sample	Compacted mass material (g)	Targets thickness (mm)
1	10.015	6.5
2	7.751	5.0
3	5.952	4.5

Table 8. Compacted mass material and target thickness.

Scanning electron microscopy (SEM) (JSM-5910LV) tests were performed on the powder material with a 36-h milling time and the material sintered at 1000°C to determine size, distribution, particle shape, and local chemical composition.

3. Results

3.1. Millings 1 and 2: wet

The diffractograms of millings 1 and 2 (**Figure 2**) show the characteristic peaks of Rutile (TiO_2), in which 2θ is equal to 28, 36, 39, and 57° approximately, and it is presented as a tetragonal structure that indicates that the largest amount of powder corresponding to the initial material. The presence of characteristic graphite peaks with a hexagonal structure, in which 2θ is equal to approximately 24, 26, and 70°, is also observed. The most representative titanium carbide peaks have a cubic structure at approximate angles of 2θ that is equal to 36, 41, 61, 72, and 91°. Also, the characteristic peaks of aluminum (Al) of cubic structure in 2θ occurred, being equal to 9, 39, and 78° approximately. Alumina peaks (Al_2O_3) with a cubic structure at 2θ equal to 13, 21, and 50° also occurred.

The diffractograms for millings 1 and 2 (**Figure 2**) showed that small amounts of TiC were formed. Milling 2, with a more milling time (7 h) was the one that had the highest intensity TiC peaks, 146 a.u. approximately and at an angle of 2θ = 36°.

3.2. Milling 3: dry and vacuum

In the diffractograms (**Figure 3**), the characteristic peaks of the Rutile phase or titanium dioxide TiO_2, the titanium carbide (TiC), and the carbon for each of the samples are observed. The titanium carbide peaks, TiC, occur with their intensity maximums in 2θ equal to 36, 41, 60, 72, and 76°. With these peaks, it was evidenced that the highest intensity occurred at the angle of 2θ being equal to 36° in sample 1, with an approximate intensity of 247 a.u.

3.3. Final milling

The diffractogram for the powders with an 18-h milling time (**Figure 4**) shows characteristic peaks of rutile, titanium carbides, mica, and hydrated elements that facilitate the formation of hydrides and carbides. The characteristic peaks of titanium carbide (TiC) occurred with an intensity of 150 a.u. at 36°, but also at 2θ being equal to 41, 60, 72, and 76°.

For the 36-h milling time, the intensity of the characteristic peak of TiC at 36° increasing to 350 a.u. was observed (**Figure 5** and **Table 7**). Peaks at 2θ being equal to 41, 60, 72, and 76° were also diffracted, which were observed in the diffractogram for the 18-h milling.

As the milling time increased, the peaks of the X-ray diffractograms widened to twice their height, evidencing a process of internal stress accumulation.

In the sintering process, it was observed that the target subjected to a 700°C sintering temperature turned to a light gray color, and when trying to take it with the tweezers to remove it

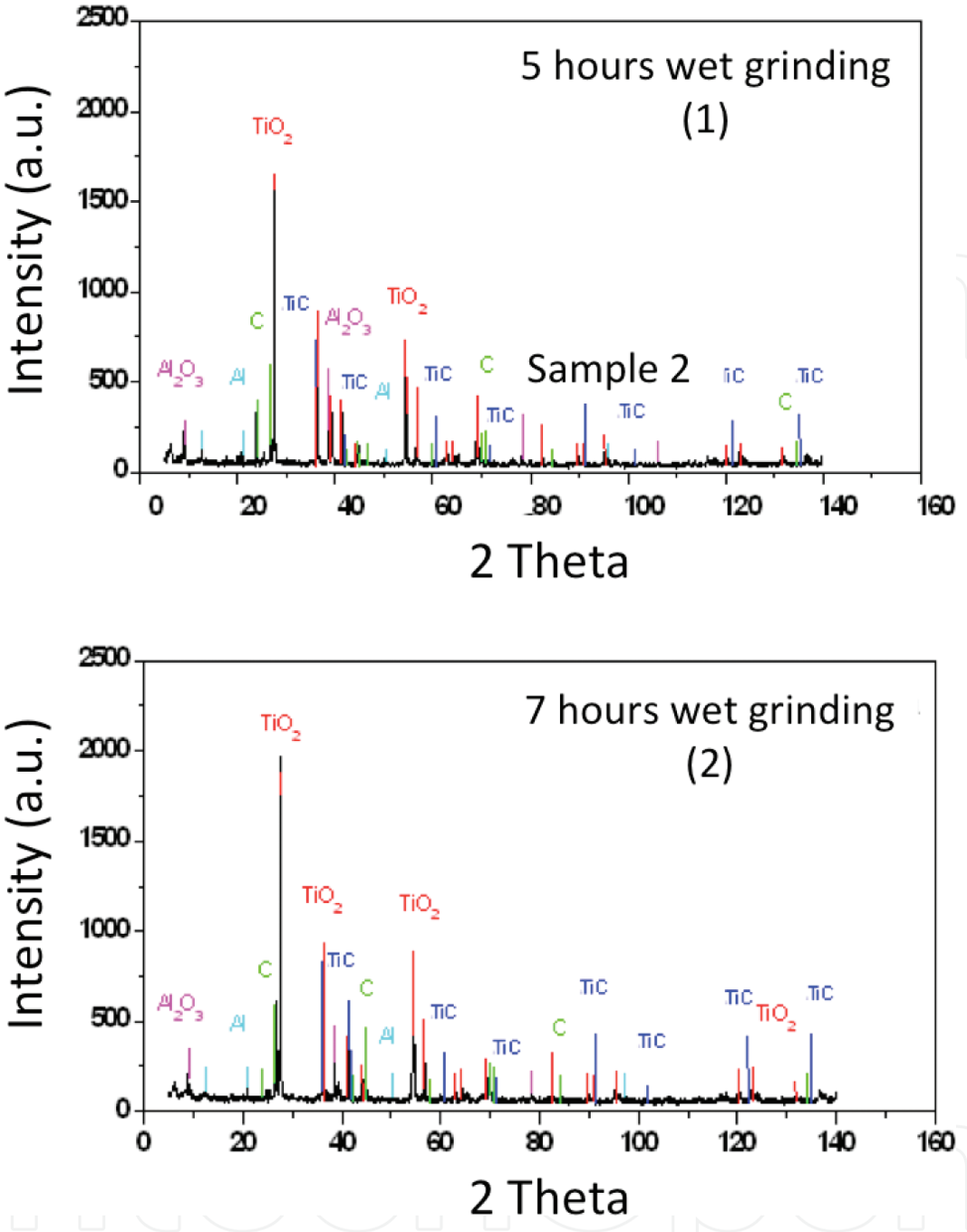

Figure 2. Diffractograms of millings 1 and 2.

from the oven, it fractured. This result shows that the material at this temperature did not sinter completely. The target subjected to a 1000°C temperature had a yellow color; this change in color is possibly due to the fact that, in the beginning, the pores are full of air, and as it was in oxidizing conditions, when opening the oven, it was discolored by the attack of oxygen on the surface [13]. This target showed a higher consistency than the sintering at 700°C.

In the micrographs (**Figure 6**) for the unsintered and 36-h milling time powders, the presence of two types of particles was observed; some of them had a spherical shape with an approximate

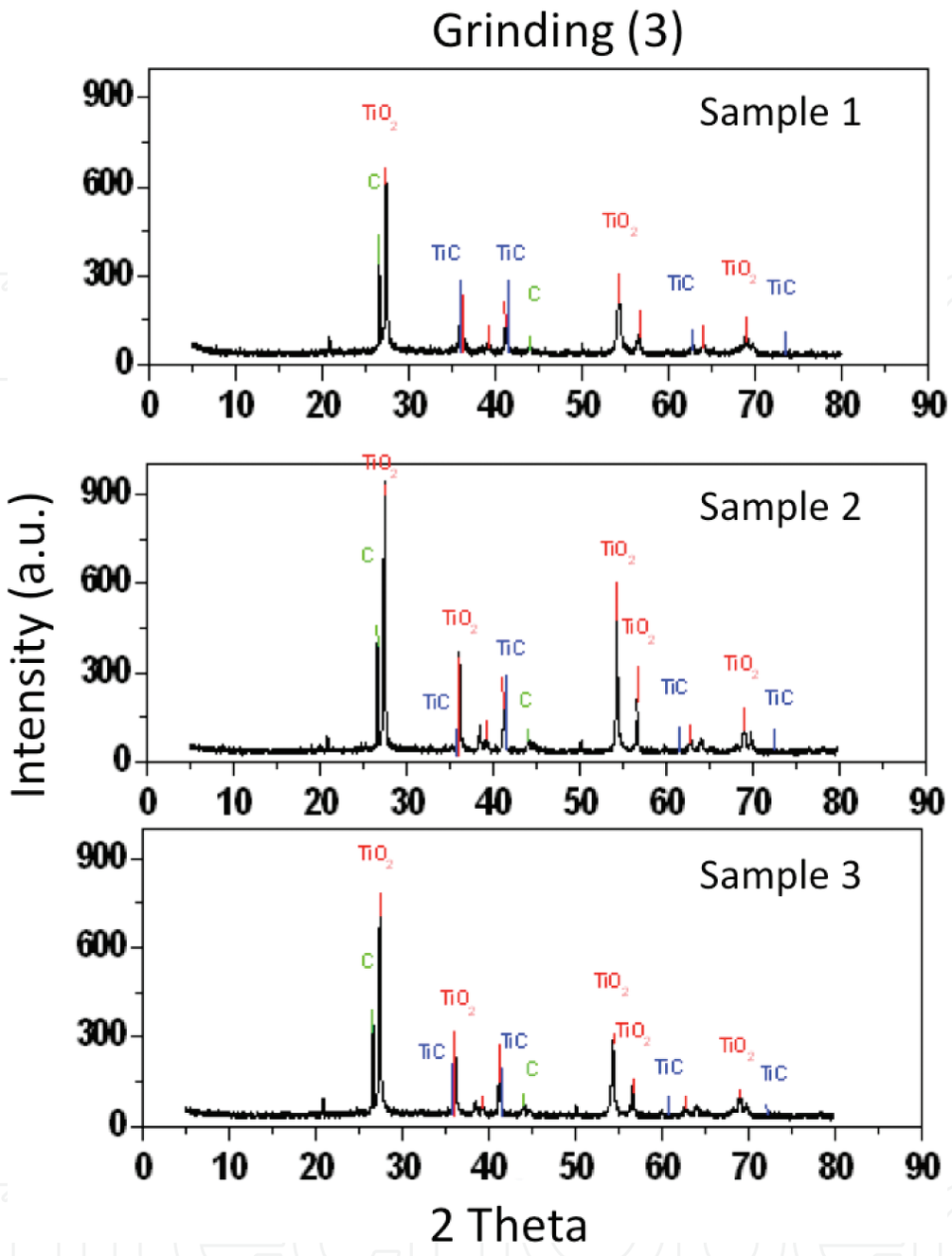

Figure 3. Diffractograms of dry and vacuum milling.

4-μm size (**Figure 6c**) and other particles of elongated shape of an approximate 1-μm size (**Figure 6e**). In general, it was found that the powders had an irregular particle size.

For the compacted and sintered material (36-h milling), a regular form of grain size was observed in the micrographs (**Figure 7**), with an average grain size of 5 μm (**Figure 7d**), and with a more regular particle size than the powder material. In the grain distribution, the growth of some grains can be seen at the expense of others, which means that a diffusion

http://dx.doi.org/10.5772/intechopen.76690

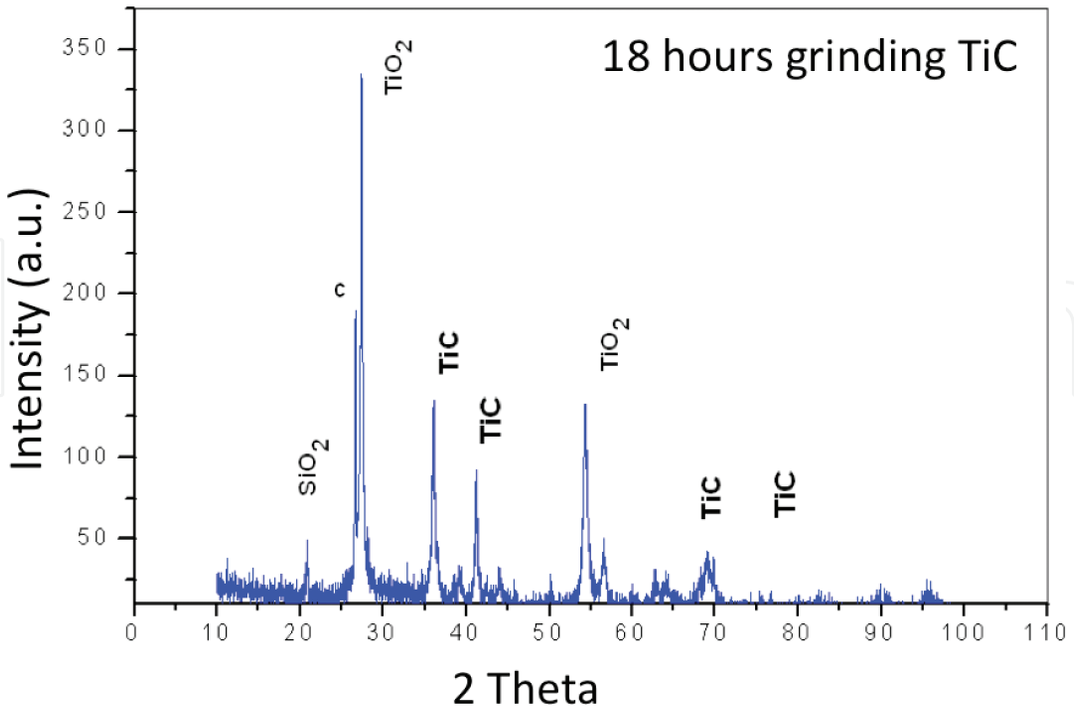

Figure 4. Diffractogram for the powders with an 18-h milling time.

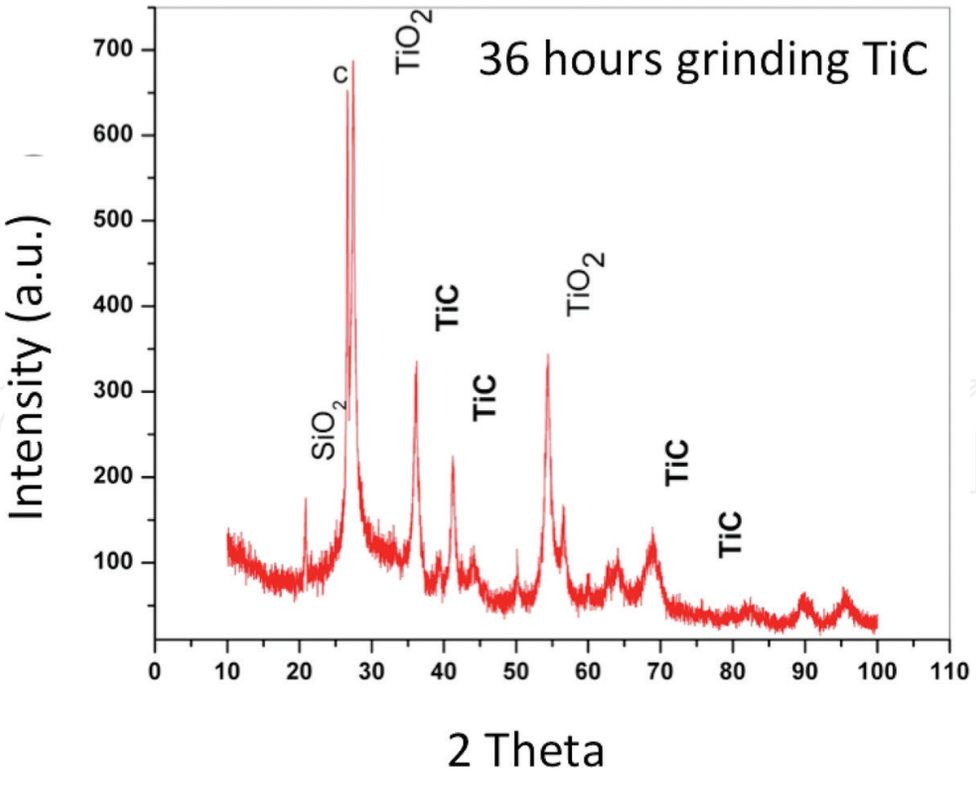

Figure 5. Diffractogram for the powders with a 36-h milling time.

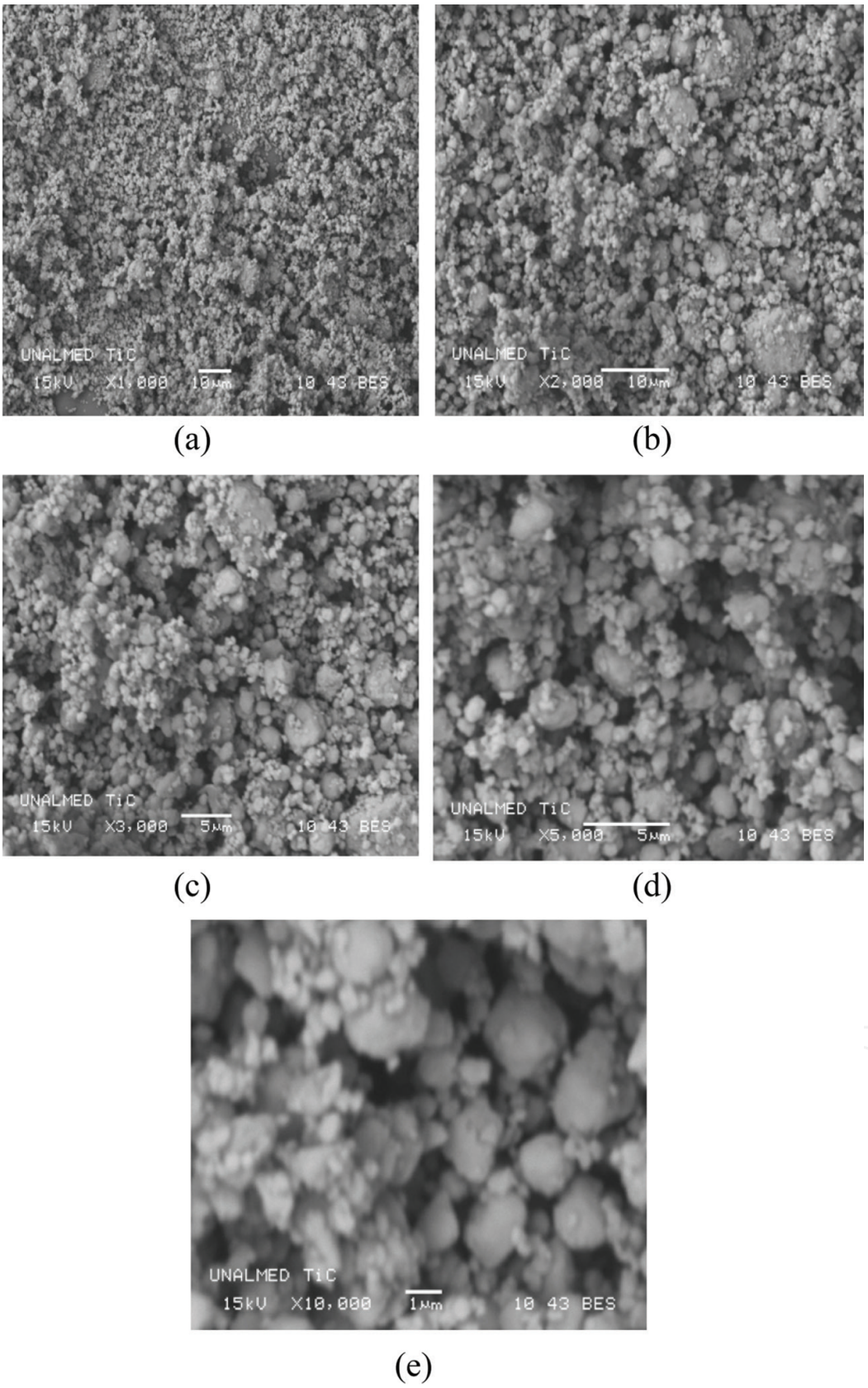

Figure 6. Micrographs for the unsintered and 36-h milling time powders: (a) 1000×, (b) 2000×, (c) 3000×, (d) 5000×, and (e) 10,000×.

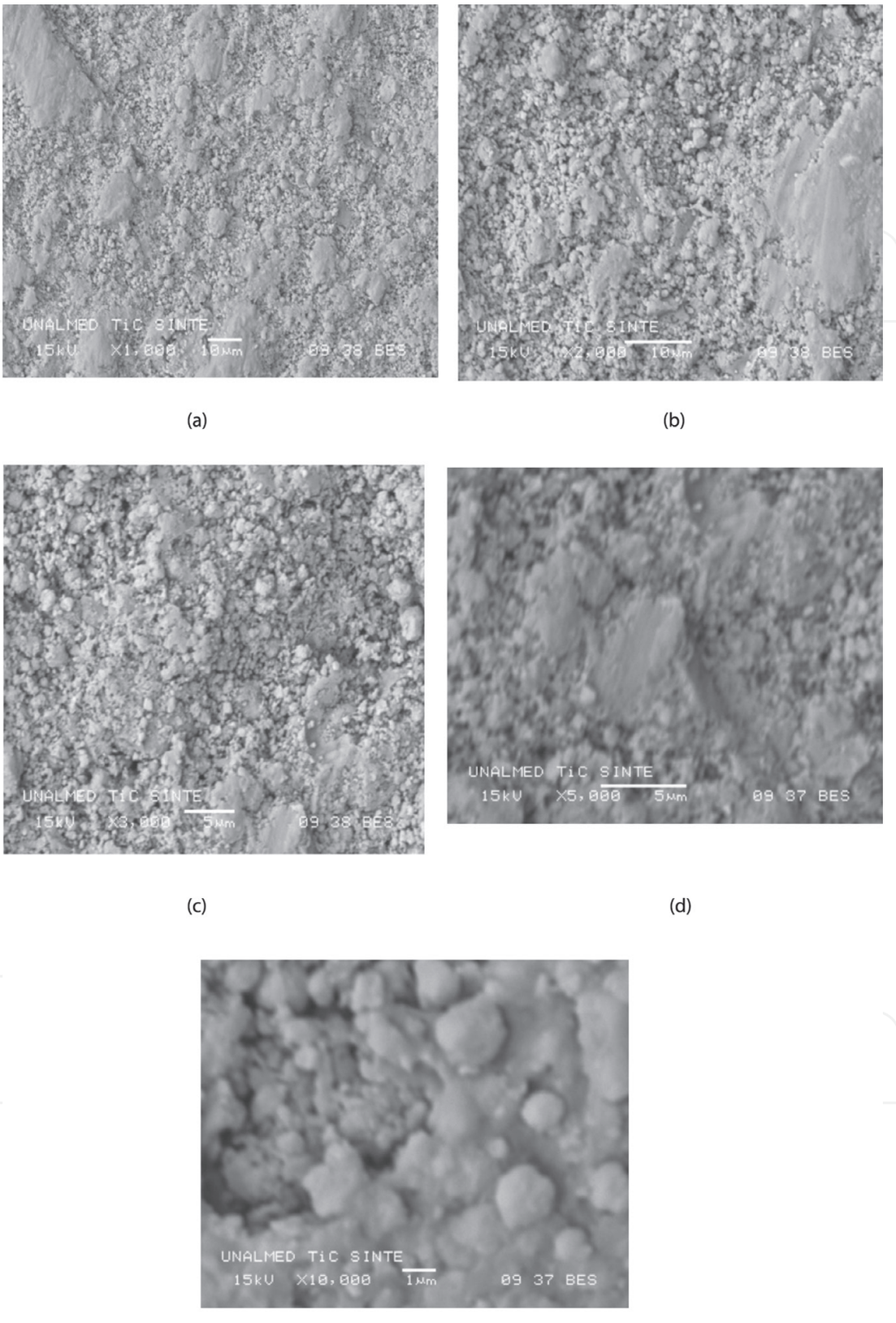

Figure 7. Micrographs for the compacted and sintered material (36-h milling): (a) 1000×, (b) 2000×, (c) 3000×, (d) 5000×, and (e) 10,000×.

process between particles occurred. The former issue showed that the 1000°C sintering favored the homogenization of grain size.

The chemical analysis performed on the powder material (36-h milling) showed the presence of elements such as silicon (Si), potassium (K), aluminum (Al), titanium (Ti), iron (Fe), and oxygen (O) (**Figure 8**). A high atomic percentage of oxygen and titanium was found (**Table 9**), which was followed by aluminum, silicon, and potassium.

For the sintered target (36-h milling), the chemical analysis (**Figure 9**) showed the presence of elements such as Al, Si, and Ti, which confirms the phases that were revealed in the X-ray diffractograms (**Figure 5**). Such present elements as calcium, potassium, and iron (**Table 10**)

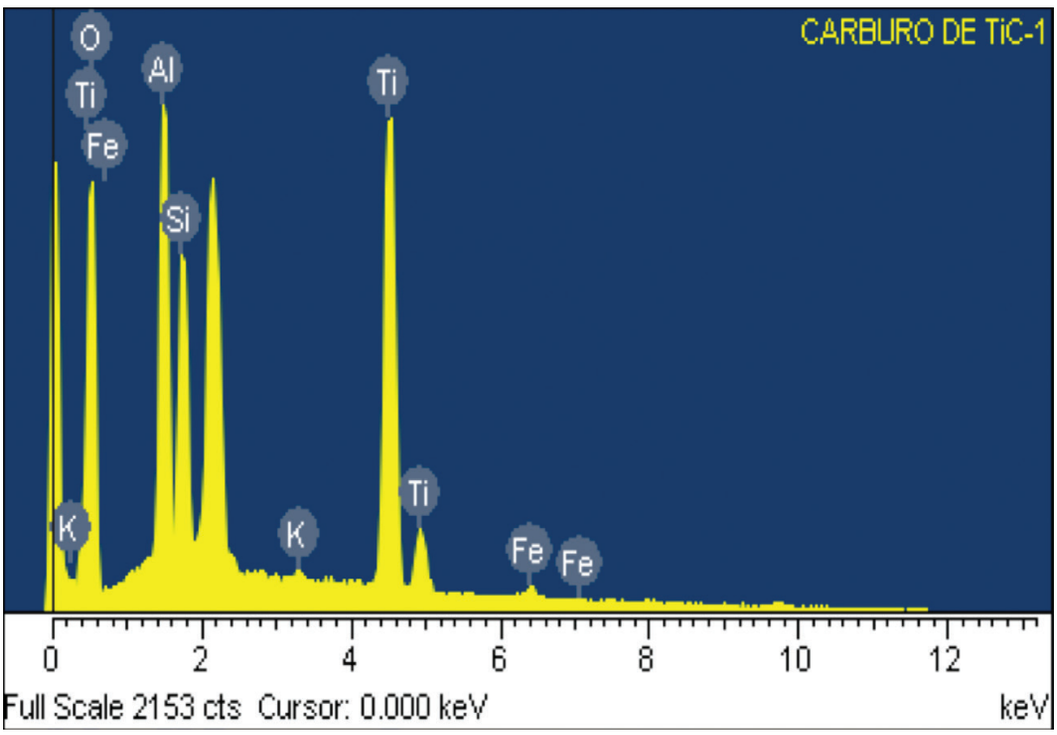

Figure 8. Scanning electron microscopy for the powder material (36-h milling).

Element	Weight (%)	Atomic (%)
O	45.89	67.14
Al	10.26	8.90
Si	7.62	6.35
K	0.33	0.20
Ti	34.00	16.62
Fe	1.90	0.80
Total	100.00	100.00

Table 9. Percentage of elements within the powders.

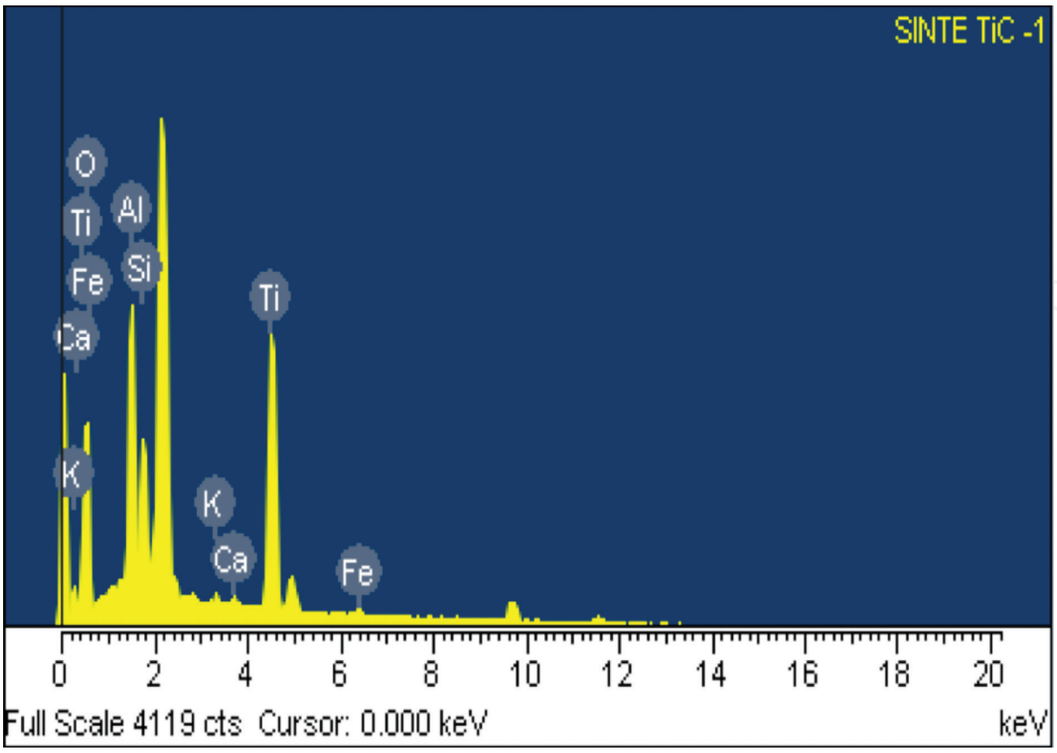

Figure 9. Scanning electron microscopy for the sintered target (36-h milling).

Element	Weight (%)	Atomic (%)
O	42.26	64.28
Al	11.61	10.39
Si	6.23	5.36
K	0.54	0.33
Ti	36.76	18.34
Fe	1.75	0.76
Ca	0.55	0.33
Total	100.00	100.00

Table 10. Percentage of elements within the sintered powders.

come from the material being found in the milling jars, as well as some impurities that the material absorbed during the sintering process.

4. Discussion

The presence of alumina in millings 1 and 2 means that the aluminum reacted with oxygen causing oxidation in the material and did not meet its main objective, which was to react with

titanium dioxide, to form titanium carbide, as was intended (Eq. (2)). The ethanol added to the mixture of millings 1 and 2, as dispersing liquid, added more oxygen to the material, making it difficult to extract the O_2 molecules from the titanium dioxide.

The highest concentration of TiC in milling 3 (sample 1), which corresponds to the powder adhered to the milling spheres, can be explained because, at this place, the highest impact energy occurs; consequently, the adhered material is in constant collision with all the parts that make up the milling bowl and this favors the creation of TiC.

The SEM micrographs of the 36-h milling powders showed a wide particle distribution, from about 200 nm through about 1 μm, while the sintered samples showed particles of spherical shape and regular distribution of grains with a size less than 5 μm. This grain distribution was produced by the growth of some grains at the expense of others, that is to say, a diffusion process occurred, and an effective sintering at a 1000°C temperature also took place.

5. Conclusions

The mechanosynthesis of titanium carbides was possible to be performed, and this is the main contribution of this research work, which uses the mechanical alloying technique from titanium dioxide, graphite, and commercial aluminum at a laboratory level.

In addition, it is necessary to highlight that the precursors being used in this process were very low cost, compared with the high-purity powders being normally used for this purpose.

Both issues open the possibility of implementing this method to obtain titanium carbides in a low-cost industrial process. Nevertheless, it is necessary to adjust the parameters of the milling process to produce TiC on an industrial scale.

Acknowledgements

This work was financed by Research and Technological Development Direction at Universidad Autónoma de Occidente, Cali, Colombia.

Author details

Héctor Enrique Jaramillo Suárez[1], Nelly Alba de Sanchez[1]* and Julian Arnaldo Avila Diaz[2]

*Address all correspondence to: nalba@uao.edu.co

1 Autónoma de Occidente University (UAO), Cali, Colombia

2 São Paulo State University (UNESP), São Paulo, Brazil

References

[1] Koch CC. The synthesis and structure of nanocrystalline materials produced by mechanical attrition: A review. Nanostructured Materials. 1993;**2**(2):109-129

[2] Murty BS, Ranganathan S. Novel materials synthesis by mechanical alloying/milling. International Materials Reviews. 1998;**43**(3):101-141

[3] DCNM by MA Techniques. New Materials by Mechanical Alloying Techniques. Oberursel: Ir Pubns Ltd; 1989

[4] Cahn RW. Materials Science and Technology, Processing of Metals and Alloys. Vol. 15. Weinheim: Wiley-VCH; 1996

[5] Zhang L, Shen H-F, Rong Y, Huang T-Y. Numerical simulation on solidification and thermal stress of continuous casting billet in mold based on meshless methods. Materials Science and Engineering: A. 2007;**466**(1):71-78

[6] Ye LL, Quan MX. Synthesis of nanocrystalline TiC powders by mechanical alloying. Nanostructured Materials. 1995;**5**(1):25-31

[7] Hack GAJ. Dispersion strengthened alloys for aerospace. Metals and Materials. 1987;**3**(457): 457-462

[8] Dossett JL, Luetje RE. Heat Treating: Proceedings of the 16th Conference. ASM International. OH, USA: ASM Press; 1996

[9] Froes FH, DeBarbadillo JJ. Structural Applications of Mechanical Alloying: Proceedings of an ASM International Conference; Myrtle Beach, South Carolina; 27-29 March 1990. ASM International; 1990

[10] Botero F, Torres JG, Jaramillo HE, de Sanchez NA, Sanchez SH. Diseño de un molino de bolas tipo atritor. Latin American Journal of Metallurgy and Materials. 2009;**S1**(4): 1423-1431

[11] El-Eskandarany MS. Mechanical Alloying: Nanotechnology, Materials Science and Powder Metallurgy. NY, USA: Elsevier Ltd; 2015

[12] Lü L, Lai MO. Mechanical Alloying. NY, USA: Springer Science & Business Media; 2013

[13] Angelo PC, Subramanian R. Powder Metallurgy: Science, Technology and Applications. New Delhi, India: PHI Learning Private Limited; 2008

IntechOpen